THE JOURNAL OF BIOLOGICAL CHEMISTRY
Vol. 280, No. 15, Issue of April 15, pp. 14385–14394, 2005
Printed in U.S.A.

Substrate Specificity, Localization, and Essential Role of the Glutathione Peroxidase-type Tryparedoxin Peroxidases in *Trypanosoma brucei**

Received for publication, November 27, 2004, and in revised form, January 12, 2005
Published, JBC Papers in Press, January 21, 2005, DOI 10.1074/jbc.M413338200

Tanja Schlecker‡, Armin Schmidt‡, Natalie Dirdjaja‡, Frank Voncken§, Christine Clayton§, and R. Luise Krauth-Siegel‡¶

From the ‡Biochemie-Zentrum der Universität Heidelberg and the §Zentrum für Molekularbiologie Heidelberg, Universität Heidelberg, 69120 Heidelberg, Germany

***Trypanosoma brucei*, the causative agent of African sleeping sickness, encodes three nearly identical cysteine homologues of the classical selenocysteine-containing glutathione peroxidases. Although one of the sequences, peroxidase III, carries both putative mitochondrial and glycosomal targeting signals, the proteins are detectable only in the cytosol and mitochondrion of mammalian bloodstream and insect procyclic *T. brucei*. The enzyme is a trypanothione/tryparedoxin peroxidase as are the 2 Cys-peroxiredoxins of the parasite. Hydrogen peroxide, thymine hydroperoxide, and linoleic acid hydroperoxide are reduced with second order rate constants of 8.7×10^4, 7.6×10^4, and 4×10^4 M^{-1} s^{-1}, respectively, and represent probable physiological substrates. Phosphatidylcholine hydroperoxide is a very weak substrate and, in the absence of Triton X-100, even an inhibitor of the enzyme. The substrate preference clearly contrasts with that of the closely related *T. cruzi* enzyme, which reduces phosphatidylcholine hydroperoxides but not H_2O_2. RNA interference causes severe growth defects in bloodstream and procyclic cells in accordance with the peroxidases being essential in both developmental stages. Thus, the cellular functions of the glutathione peroxidase-type enzymes cannot be taken over by the 2 Cys-peroxiredoxins that also occur in the cytosol and mitochondrion of the parasite.**

The causative agents of African sleeping sickness (*Trypanosoma brucei gambiense* and *T. brucei rhodesiense*), Nagana cattle disease (*Trypanosoma congolense*, *T. brucei brucei*), South-American Chagas' disease (*Trypanosoma cruzi*), and the different forms of leishmaniasis, differ from all other known eukaryotes and prokaryotes in their unique thiol redox system. The thiol-polyamine conjugate trypanothione (N^1,N^8-bis(glutathionyl)spermidine) (1) and the flavoenzyme trypanothione reductase (TR)[1] replace the nearly ubiquitous glutathione/glutathione reductase system. A direct linkage between glutathione and spermidine metabolism was first discovered in *Escherichia coli* (2). During stationary phase, all of the cellular spermidine and a large part of glutathione occur as mono(glutathionyl)-spermidine whereby the bacterium does not form trypanothione. The dithiol trypanothione is the donor of reducing equivalents for the reduction of thioredoxin (3), the synthesis of deoxyribonucleotides by ribonucleotide reductase (4), protein biosynthesis (5), and the replication of kinetoplastid DNA (6) as well as the detoxification of ketoaldehydes (7) and hydroperoxides (for recent reviews, see Refs. 8 and 9). Trypanosomes are exposed to various reactive oxygen species such as superoxide anions, hydrogen peroxide, and products of the host myeloperoxidase system. However, their ability to cope with oxidative stress is relatively weak. Although the parasites possess superoxide dismutase, they lack catalase and selenocysteine-containing glutathione peroxidases, the main hydroperoxide-metabolizing enzymes in the mammalian host. In trypanosomatids, three classes of peroxidases, 2 Cys-peroxiredoxins (9–11), cysteine-homologues of the classical glutathione peroxidases (12–14), and an ascorbate-dependent hemoperoxidase (15), have been characterized that all obtain their reducing equivalents from trypanothione. The enzymatic cascades for the 2 Cys-peroxiredoxins and the glutathione peroxidase-type peroxidases are identical. With NADPH as the final electron donor, the reducing equivalents flow via trypanothione onto tryparedoxin and finally the peroxidase, which then catalyzes the reduction of the hydroperoxide (9–11, 13, 14, 16). This means that the 2 Cys-peroxiredoxins and the glutathione peroxidase-type enzymes act as trypanothione-dependent tryparedoxin peroxidases.

In *T. cruzi*, the genes of two cysteine homologues of glutathione peroxidases have been cloned and overexpressed. One of the enzymes has been described as *T. cruzi* glutathione peroxidase I, but the reported activities with glutathione were extremely low (12). Later the enzyme was also shown to use the trypanothione/tryparedoxin couple as an electron source (13). The *T. cruzi* peroxidase catalyzes the reduction of different hydrophobic substrates, especially of phospholipid hydroperoxides such as phosphatidylcholine hydroperoxide but not of hydrogen peroxide. In African trypanosomes, a genomic locus encodes three nearly identical glutathione peroxidase-type enzymes (14). RNA interference approaches revealed that the enzyme(s) is essential for the viability of bloodstream *T. brucei* (17). Although *T. cruzi* glutathione peroxidase I and the *T. brucei* peroxidases share 72% of all residues, they show significant differences in their cellular localization as well as their kinetic properties as will be outlined here.

Four types of selenocysteine-containing glutathione peroxidases have been characterized in mammals, the cytosolic cGPX

* This work was supported by Deutsche Forschungsgemeinschaft, Sonderforschungsbereich 544 "Control of Tropical Infectious Diseases," project B3. The costs of publication of this article were defrayed in part by the payment of page charges. This article must therefore be hereby marked "*advertisement*" in accordance with 18 U.S.C. Section 1734 solely to indicate this fact.

¶ To whom correspondence should be addressed: Biochemie-Zentrum der Universität Heidelberg, Im Neuenheimer Feld 504, 69120 Heidelberg, Germany. Tel.: 49-6221-544187; Fax: 49-6221-545586; E-mail: krauth-siegel@urz.uni-heidelberg.de.

[1] The abbreviations used are: TR, trypanothione reductase; ROOH, hydroperoxide; GPX, glutathione peroxidase; PhGPX, phospholipid hydroperoxide glutathione peroxidase; Px, glutathione peroxidase-type tryparedoxin peroxidase (Cys homologue of glutathione peroxidase); Pex, peroxin; BiP, endoplasmic reticulum chaperon (binding protein).

(GPX I), also called classical or cellular glutathione peroxidase, the gastrointestinal GI-GPX (GPX II), the extracellular pGPX (GPX III) found in human plasma, and the phospholipid hydroperoxide glutathione peroxidase (PhGPX) (GPX IV). The cytosolic glutathione peroxidase uses glutathione as reducing substrate, whereas the extracellular enzyme accepts thioredoxin and glutaredoxin and PhGPX can be reduced by a variety of protein thiols (18, 19). Selenocysteine-containing glutathione peroxidases have so far only been found in vertebrates and a GPX IV type enzyme in the helminth *Schistosoma mansoni* (20). In contrast, genes encoding cysteine homologues such as the *T. cruzi* and *T. brucei* peroxidases are widely distributed in nature. Only a few of these enzymes have been functionally characterized. All of them have much lower peroxidase activities than the mammalian seleno-enzymes (14, 21). A cysteine homologue from the malarial parasite *Plasmodium falciparum* reduces H_2O_2 but not at all phosphatidylcholine hydroperoxide and proved to be much more efficient with thioredoxin than with glutathione as the electron source (21). An enzyme from the nematode *Brugia pahangi* reduces linoleic acid hydroperoxide and phosphatidylcholine hydroperoxide but not H_2O_2 with glutathione as the reducing substrate. It is a secreted glycoprotein, and the natural electron source is not known (22).

Here we will report on the substrate specificity and subcellular occurrence of the *T. brucei* glutathione peroxidase-type enzymes. African trypanosomes multiply as bloodstream parasites in the mammalian host and as procyclic parasites in the tsetse fly. Cell fractionation studies revealed the proteins in the cytosol and the mitochondrion of both cell types. No peroxidase was detectable in glycosomes, although one protein sequence contains a putative glycosomal/peroxisomal targeting signal. Hydrogen peroxide, thymine hydroperoxide, and linoleic acid hydroperoxide are probable physiological substrates of the *T. brucei* peroxidase. The results of RNA interference experiments demonstrated that the enzyme is also essential for procyclic in addition to bloodstream *T. brucei*.

EXPERIMENTAL PROCEDURES

Materials—The recombinant glutathione peroxidase-type *T. brucei* tryparedoxin peroxidase (14), *T. brucei* tryparedoxin (23), and *T. cruzi* trypanothione reductase (24) were prepared as described. Polyclonal rabbit antibodies against the recombinant His-tagged *T. brucei* peroxidase III (14), *T. brucei* tryparedoxin (25), and *T. cruzi* trypanothione reductase were produced by Bioscience, Göttingen, Germany and Eurogentec, Belgium, respectively. The TR antibodies were purified by affinity chromatography on recombinant *T. cruzi* TR.[2] Polyclonal rabbit antibodies against the *T. brucei* homologue of the endoplasmic reticulum matrix protein BiP were a kind gift of Dr. James Bangs, Madison, WI. Other polyclonal rabbit antibodies used in this study were directed against the *T. brucei* glycosomal membrane protein Pex11 (26) and against *T. cruzi* lipoamide dehydrogenase, a mitochondrial matrix enzyme (27). Phosphatidylcholine hydroperoxide and a rat sperm preparation with phospholipid hydroperoxide glutathione peroxidase (PhGPX) were kindly provided by Dr. Regina Brigelius-Flohé, German Institute of Human Nutrition, Potsdam, Germany. Thymine hydroperoxide was synthesized according to a published procedure (28). Trypanothione disulfide was purchased from Bachem, H_2O_2 was from Merck. *t*-Butyl hydroperoxide, linoleic acid, and soybean lipoxygenase were from Sigma. All other chemicals were of the highest available purity.

Preparation of Recombinant Tag-free T. brucei Peroxidase III—Stored purified His_6-Px III as well as the run-through of the nickel column used for purification showed significant amounts of a truncated tag-free protein species with identical specific activity but a 2-kDa lower molecular mass. Edman degradation of the protein yielded (K)K-MSAA as the N-terminal sequence (14). The tag-free Px III was purified from the flow-through of the metal chelator column. Ammonium sulfate was added at 40% saturation. After centrifugation the pellet was discarded, and the saturation in the supernatant was raised to 65%. After centrifugation, the precipitate was dissolved in 100 mM Tris, 1 mM EDTA, pH 7.6, filtered through a 0.2-μm filter (Schleicher & Schuell), and loaded onto a Superdex 75 HiLoad 26/60 column (Amersham Biosciences). Approximately 80 mg of total protein in 2 ml of buffer was applied onto the column equilibrated in 100 mM Tris, 1 mM EDTA, pH 7.6. The fast protein liquid chromatography was run at room temperature at a flow rate of 2.0 ml/min, and 2-ml fractions were collected. The peroxidase-containing fractions were pooled. The protein solution was concentrated using an Amicon ultra 10000 MWCO concentrator (Millipore) to about 1 mg/ml and stored at 4 °C. The purity was more than 90%.

Synthesis of Linoleic Acid Hydroperoxide—Linoleic acid hydroperoxide was synthesized enzymatically by modification of a published protocol (29). Linoleic acid (16 μmol) was dissolved in 0.5 ml of ethanol. 0.1 M sodium borate buffer, 0.5 mM EDTA, pH 10, was added to give a total volume of 32 ml and a final concentration of 240 μM linoleic acid. 42 μg of soybean lipoxygenase was added, and hydroperoxide formation was monitored at 235 nm ($\epsilon = 25\ mM^{-1}\ cm^{-1}$). After 20 min of incubation at 4 °C, the lipoxygenase was removed by centrifugation through Amicon ultra 10000 MWCO concentrators (Millipore). The linoleic acid hydroperoxide was freed from the borate buffer by ether extraction and dried in an argon stream. The pellet was re-dissolved in 100% ethanol to a final concentration of 3 mM, and the solution was stored at 4 °C for up to 7 days.

Peroxidase Standard Assay—The trypanothione/tryparedoxin-dependent peroxidase activity of Px III was followed at 25 °C in a total volume of 150 μl of 0.1 M Tris, 5 mM EDTA, pH 7.6, containing 240 μM NADPH, 100 μM trypanothione disulfide, 150 milliunits of TR, 10 μM tryparedoxin, and 0.05 μM peroxidase in the case of thymine hydroperoxide and 0.11 μM enzyme when H_2O_2 or linoleic acid hydroperoxide and 0.5 μM peroxidase when *t*-butyl hydroperoxide or phosphatidylcholine hydroperoxide were studied as substrates. The reaction was started by adding 100 μM hydroperoxide substrate, and NADPH consumption was followed at 340 nm. The total concentration of hydroperoxide in the assay was determined by allowing the reaction to run to completion. Reduction of phosphatidylcholine hydroperoxide by rat PhGPX was measured as the control.

Kinetic Analysis of Different Hydroperoxide Substrates—The assays contained in a total volume of 150 μl of 0.1 M Tris, 5 mM EDTA, pH 7.6, 240 μM NADPH, 100 μM trypanothione disulfide, 150 milliunits of TR, 1–10 μM tryparedoxin, and 0.4 or 1.5 μM peroxidase when thymine hydroperoxide and linoleic acid hydroperoxide were studied as the substrate, respectively. The reaction was started by adding 50 μM hydroperoxide. Concentration dependence of the initial velocities was obtained by analyzing the time progression curve of NADPH consumption in a Beckman DU65 spectrophotometer with data acquisition every 1.5 s. The data were analyzed using the integrated Dalziel equation for a two-substrate enzyme reaction (30, 31) (Equation 1),

$$\frac{[E]_t}{[ROH]_t} = \phi_0 + \phi_1 \frac{\ln \frac{[ROOH]}{[ROOH]-[ROH]_t}}{[ROH]_t} + \phi_2 \frac{1}{[Thiol]} \qquad \text{(Eq. 1)}$$

where [ROOH] is the initial hydroperoxide concentration, $[ROH]_t$ is the concentration of the product at a time *t*, [Thiol] the concentration of tryparedoxin, [*E*] the total concentration of the peroxidase, and Φ_0, Φ_1, and Φ_2 are the kinetic Dalziel coefficients (30, 31) as described in Hillebrand *et al.* (14).

Cultivation of Bloodstream and Procyclic T. brucei—For all experiments described here, culture-adapted bloodstream and procyclic *T. brucei* of cell line 449 were used. The cells are descendents of strain Lister 427 (32) that were stably transfected with pHD449 encoding the tetracycline repressor (33). Bloodstream *T. brucei* were grown at 37 °C in a humidified atmosphere with 5% CO_2 in HMI-9 medium supplemented with 1.5 mM cysteine, 0.0014% (v/v) β-mercaptoethanol, 10% heat-inactivated fetal calf serum (v/v), 50 units/ml penicillin, 50 μg/ml streptomycin, and 0.2 μg/ml phleomycin to select for cells containing the tet repressor. Procyclic *T. brucei* were grown in MEM-Pros medium (Biochrom) supplemented with 7.5 μg/ml hemin, 10% heat-inactivated fetal calf serum (v/v), 50 units/ml penicillin, 50 μg/ml streptomycin, and 0.5 μg/ml phleomycin at 27 °C.

Quantification of the Peroxidase in Bloodstream and Procyclic T. brucei—2×10^6 exponential-phase procyclic and bloodstream trypanosomes were harvested by centrifugation at 2000 × *g*. The cell pellets were mixed with 20 μl of 2× Laemmli buffer (125 mM Tris, pH 6.8, 4% (v/v) SDS, 20% (v/v) glycerol, 25 mM dithioerythritol, 0.02% (w/v) bromphenol blue) and directly loaded onto a 15% SDS-polyacrylamide gel. 7, 14, 28, and 56 ng of tag-free Px III was applied onto the

[2] S. Meiering and R. L. Krauth-Siegel, unpublished work.

same gel. After electrophoresis, the proteins were transferred onto a Hybond™-P membrane (Amersham Biosciences) by wet electroblotting and probed with the polyclonal rabbit antiserum against the recombinant peroxidase (dilution 1: 2000). Anti-rabbit IgG (dilution 1:20,000, Santa Cruz Biotechnology) served as secondary antibody. The immune complex was visualized by the SuperSignal® West Pico chemiluminescent substrate (Pierce). The intensity of the protein bands was quantified by the program Gel Pro Analyzer 3.1 as absolute integrated optical density.

Subcellular Localization of the Peroxidase in Procyclic and Bloodstream T. brucei—A sucrose gradient was prepared following a modified protocol of Opperdoes *et al.* (34). 1×10^{10} parasites were collected by centrifugation at $800 \times g$ and 4 °C. The cell pellet was washed with TEDS buffer (25 mM Tris, 1 mM EDTA, 1 mM dithiothreitol, 250 mM sucrose, pH 7.8), resuspended in TEDS, 15% glycerol, and frozen at −80 °C. The cells were thawed at room temperature and washed in TEDS, a protease inhibitor mixture (Complete Mini, Roche Applied Science) dissolved in 2–3 ml TEDS was added, and the cells were manually broken with silicon carbide (Merck). The silicon carbide was removed by centrifugation at $100 \times g$, and the supernatant was loaded on top of a 39-ml semi-continuous 30–60% sucrose gradient, with a 68% sucrose cushion and 30% sucrose as the top concentration. Separation of the different cell compartments was achieved by centrifugation at $170{,}000 \times g$ and 4 °C in a vertical rotor (Beckman VTi50) for 1 h in an ultracentrifuge (Beckman). 700-μl fractions were collected from the bottom of the centrifuge tube, and the protein concentration in each fraction was determined using the bicinchoninic acid kit (Pierce). To 250 μl of each fraction trichloroacetic acid and deoxycholate were added at 20% (w/v) and 0.4% (w/v) concentrations, and the mixture was incubated overnight at 4 °C. After a 15-min centrifugation at 13,000 rpm (Eppendorf centrifuge 5810R), the protein pellet was washed with 100% acetone, dissolved in 50 or 25 μl of 1× Laemmli buffer, and boiled for 2 min. For the bloodstream cells 8 μl of the 5 times-concentrated gradient fractions were applied on 10 or 15% SDS gels. In the case of the procyclic parasites, 20-μl aliquots of the 10 times-concentrated gradient fractions were analyzed. Western blots were performed as described above with the polyclonal rabbit antiserum against the recombinant peroxidase (dilution 1:2000). To distinguish the different cell compartments, the blots were developed with antibodies directed against the marker proteins Pex11 (1:1000), lipoamide dehydrogenase (1:1000), BiP (1:2000), and TR (1:500). Anti-rabbit IgG (dilution 1: 20,000, Santa Cruz) served as secondary antibody.

RNA Interference Constructs and Transfection—A 452-bp fragment of the peroxidase III-coding region was amplified twice from genomic DNA of procyclic *T. brucei* strain AnTaT 1.1. Px-s (5′-GCA ACA T*AA GCT T*CA ATC TTT GAC TTT GAG GTG C-3′, the HindIII restriction site is given in italics) and Px-R-s-II (5′-GCA ACA T*GT TAA C*CA ATC TTT GAC TTT GAG GTG C-3′, HpaI site), respectively, served as forward primers. Px-as (5′-CA*G AAT TCT GCA G*CT CAA TAT CCT TCA CAG AGG-3′, overlapping EcoRI and PstI sites are given in italics) was used as the reverse primer in both polymerase chain reactions. The fragments were cloned into the HindIII/PstI and EcoRI/HpaI restriction sites, 5′ and 3′ of the stuffer segment in a vector derived from pSP72 (35). The two gene copies together with the stuffer sequence were then ligated as HindIII/HpaI-digested cassette into the tetracycline-inducible vector pHD678 containing a hygromycin resistance gene (33). The construct pHD678*px* targets the transcripts of the three nearly identical peroxidase genes (14). 10^7 Procyclic and bloodstream *T. brucei* of strain 449 were transfected by electroporation with 10 and 30 μg, respectively, of the NotI-linearized plasmid DNA and selected for hygromycin resistance (50 μg/ml) as described by Wang *et al.* (36). Procyclic and bloodstream cells were harvested at a maximum density of 5×10^6 and 1×10^6 cells/ml, respectively. Bloodstream transfectants were seeded in 25 ml of HMI-9 medium containing 0.2 μg/ml phleomycin, and 1-ml aliquots were placed in a 24-well microtiter plate. After incubation overnight, 1 ml of fresh medium containing 0.2 μg/ml phleomycin and 10 μg/ml hygromycin were added to each well. Transfected procyclic *T. brucei* were seeded in 5 ml of MEM-Pros medium with 0.5 μg/ml phleomycin and allowed to grow overnight. After adding another 5 ml of fresh medium containing 0.5 μg/ml phleomycin and 100 μg/ml hygromycin, the cells were again incubated overnight. The culture was then diluted with conditioned medium containing 50 μg/ml hygromycin and subjected to serial dilutions into 6 wells of about 1×10^6, 3×10^5, 1×10^4, and 5×10^3 cells/ml. Bloodstream and procyclic cells were grown for 2 weeks before clones were harvested. Bloodstream clones were cultivated in the presence of 0.2 μg/ml phleomycin and 5 μg/ml hygromycin, the procyclic clones in the presence of 0.5 μg/ml phleomycin and 50 μg/ml hygromycin.

Growth Phenotypes—To follow cell growth under continuous cultivation, 2×10^5 bloodstream trypanosomes per ml transformed with pHD678*px* were mixed with 0.5 μg/ml tetracycline and grown for 72 h. To determine the growth behavior upon cultivation in 24 h cycles, 1×10^5 bloodstream cells/ml were induced with 1 μg/ml tetracycline, and every 24 h the cultures were diluted with the tetracycline-containing medium to 1×10^5 cells/ml as required. In transfected procyclic parasites, RNA interference was induced by adding 1 μg/ml tetracycline at a cell density of 4×10^5 cells/ml for continuous cultivation and at 1×10^6 cells/ml for the cultivation in 24-h cycles. The cells were counted in a Neubauer chamber. For comparison, wild type cells of strain 449 were grown in the absence of tetracycline, and cells of strain 449 transfected with the empty plasmid pHD678 were grown with and without tetracycline.

Preparation of T. brucei Total RNA and Northern Blot Analysis—Total RNA from tetracycline-induced and non-induced *T. brucei* cells of procyclic and bloodstream strains 449 ($5 \times 10^8 - 1 \times 10^9$ cells) was prepared with the RNeasy kit (Qiagen). Total RNA was separated on a 1% agarose gel containing 1.8% formaldehyde, blotted onto a Hybond™-N^+ membrane (Amersham Biosciences), and hybridized with the digoxigenin-labeled peroxidase gene. The luminescence probe was obtained by polymerase chain reaction with the Px-s and Px-as primers (see above) and pHD678*px* as template. Tubulin served as a loading control. The luminescence probe was amplified from the pHD887 plasmid template with primers β-Tub-s (5′-GAC CGT ATC ATG ATG ACT TTC-3′) and β-Tub-as (5′-CTT CAT TAC CTA CTG CTA ATG-3′). The mRNAs were visualized with the digoxigenin DNA labeling and detection kit (Roche Applied Science).

Western Blot Analysis of the RNA Interference Clones—Tetracycline-induced and non-induced cells (2×10^6 procyclic and bloodstream trypanosomes grown in 24-h cycles) were harvested by centrifugation at $2000 \times g$. The cell pellets were mixed with 20 μl of 2× Laemmli buffer, boiled, and directly loaded onto a 15% SDS-polyacrylamide gel. The Western blot was performed as described above with the polyclonal rabbit antiserum against the recombinant peroxidase (1:1000). Subsequently the membrane was stripped with 62.5 μM Tris, 2% SDS (w/w), 0.1 M β-mercaptoethanol for 30 min at 60 °C and incubated with antibodies against trypanothione reductase as described above.

RESULTS

Substrate Specificity—T. brucei peroxidase III has previously been shown to catalyze the trypanothione/tryparedoxin-dependent reduction of H_2O_2, *t*-butyl hydroperoxide, and cumene hydroperoxide (14). The aim of this study was to reveal probable physiological substrates of the enzyme and to compare its substrate specificity with that of a homologous *T. cruzi* peroxidase (12, 13) as well as the mammalian PhGPX (37), which represents the structurally closest related host enzyme. Reduction of thymine hydroperoxide and linoleic acid hydroperoxide by peroxidase III was studied by single curve progression analysis according to Forstrom *et al.* (31) using the integrated Dalziel equation (Equation 1) as outlined in Hillebrand *et al.* (14). The hydroperoxide concentration was chosen such that the reaction rate was dependent on its concentration. The thiol concentration was kept constant over time by coupling the reaction to that of trypanothione reductase, which allowed the reactions to be followed by measuring NADPH consumption. As shown in Fig. 1*A* for thymine hydroperoxide, the integrated reciprocal initial velocities multiplied by the enzyme concentration were plotted against the integrated reciprocal concentrations of the hydroperoxide substrate. The slope of this primary plot is the Dalziel coefficient Φ_1, which corresponds to the reciprocal of rate constant k_1 for the reduction of the peroxide (see the legend of Table I). A re-plot of the ordinate intercepts, which represent the reciprocal apparent maximum velocities at infinite peroxide concentration against the reciprocal tryparedoxin concentration, yielded a straight line that cut the ordinate at Φ_0 (Fig. 1*B*). This means that the enzyme does not show saturation at high concentrations of both substrates but that the limiting V_{max} and K_m values are infinite. The kinetic pattern can be due to two distinct catalytic phenomena. Either formation of enzyme-substrate complexes

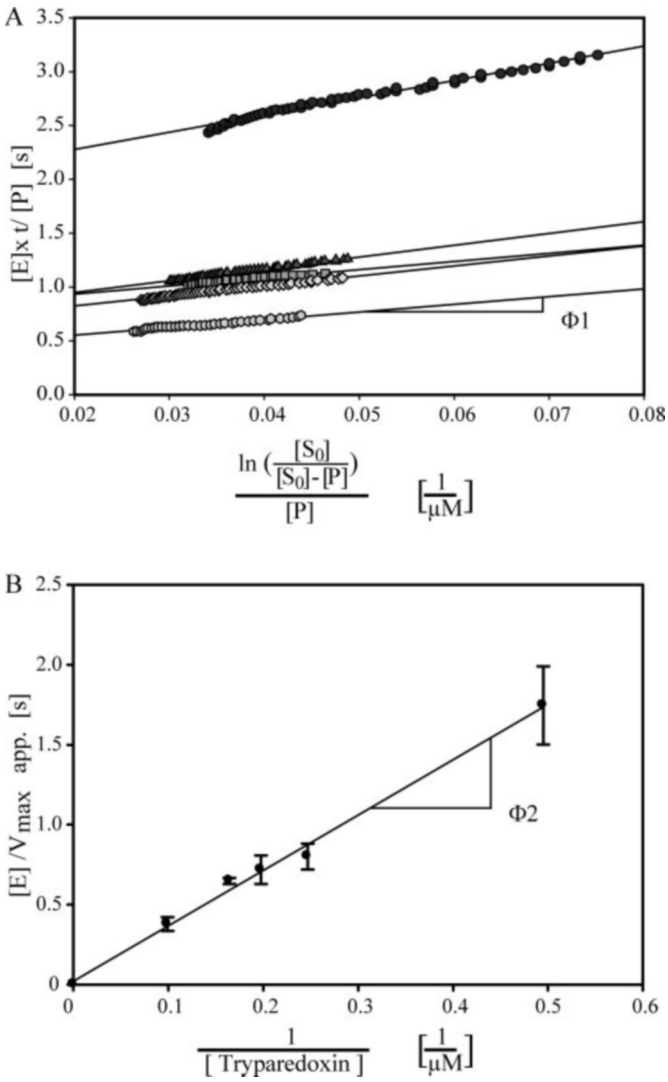

FIG. 1. **Kinetic analysis of the peroxidase-catalyzed reduction of thymine hydroperoxide.** The activities were measured at a fixed concentration of 100 μM trypanothione and 2 (●), 4 (▲), 5 (*gray box*), 6 (*gray diamond*), and 10 (*gray hexagon*) μM tryparedoxin as described under "Experimental Procedures." *A*, primary Dalziel plot. The hydroperoxide concentration at each time point was obtained by single curve progression analysis (31). The empirical Dalziel coefficient Φ_1 is given by the slope of the linear regressions. The *ordinate* $[E] \times t/([S_0] - [S])$ represents $[E]/v$, and the *abscissa* is equivalent to 1/[ROOH]. $[E]$ is the enzyme concentration, and $[S_0]$ and $[S]$ are the peroxide concentrations at time point zero and the respective time. $[P]$ is $[S_0] - [S]$, the concentration of the product at a given time point. *B*, secondary Dalziel plot. The slope represents the Dalziel coefficient Φ_2 and the *ordinate* intercept corresponds to Φ_0. Intersecting the ordinate at zero implies that the apparent maximum velocity ($V_{max\ app.}$) and K_m are infinite for the respective substrate pair. The regression curves were obtained using Excel. For details see the legend of Table I.

is slower than the reaction within the complexes, or specific enzyme-substrate complexes are not formed at all (21). The slope of the secondary plot represents the Dalziel coefficient Φ_2 which corresponds to the reciprocal of the rate constant k_2 for the two-step regeneration of the reduced peroxidase (Table I). Thymine hydroperoxide is an excellent substrate of the *T. brucei* peroxidase III. It is reduced with a second order rate constant comparable to that for H_2O_2. Linoleic acid hydroperoxide is also reduced by Px III but at half that rate. In the absence of detergents phosphatidylcholine hydroperoxide is a very poor substrate, and it was not possible to determine the rate constants for its reduction as described above. To directly compare the reactivity of the peroxidase toward the different hydroperoxide substrates, standard assays were performed measuring initial ΔA/min at fixed concentrations of trypanothione/tryparedoxin and hydroperoxide (Table II). As expected, thymine hydroperoxide and H_2O_2 are efficient substrates, linoleic acid hydroperoxide and *t*-butyl hydroperoxide are reduced at lower rates, and phosphatidylcholine hydroperoxide is almost not reduced. Moreover, Px III is inactivated by the latter compound. Preincubation of the enzyme with 30 μM phosphatidylcholine hydroperoxide for 30 min before starting the reaction by adding 80 μM H_2O_2 lowered the enzyme activity to ≤5% of an untreated enzyme sample. When the parasite enzyme was treated with 80 μM phosphatidylcholine hydroperoxide in the presence of 0.5% Triton X-100 (8.45 mM) for 30 min, the activity with 100 μM H_2O_2 remained at 80% of the control. Preincubation of peroxidase III with H_2O_2 did not cause any inactivation excluding a general substrate inactivation. In the presence of 0.1% Triton X-100, phosphatidylcholine hydroperoxide is reduced by peroxidase III but is still the poorest substrate (Table II). Phosphatidylcholine hydroperoxide preparations may contain up to 2% deoxycholate,[3] which is equivalent to a final concentration of ≤2 μM in a standard assay with 100 μM phosphatidylcholine hydroperoxide. Because deoxycholate has been shown to strongly influence the activity of mammalian PhGPX (38) 4.5 μM Px III was preincubated with up to 33 mM deoxycholate for 30 min, and then the activity was measured with 100 μM H_2O_2 in a standard assay. With ≤21 μM deoxycholate in the assay, no effect on the enzyme activity was observed. Thus, inhibition of Px III was caused by phosphatidylcholine hydroperoxide and is not due to the possible presence of deoxycholate. Because Px III showed higher activity toward all hydroperoxides in the presence of the detergent, control assays contained 0.1% and 0.3% Triton X-100 but no hydroperoxide. No peroxidase activity was detectable excluding the presence of Triton X-100 hydroperoxides, which might have functioned as substrates (39). The reasons for the higher activity of peroxidase III in the presence of Triton X-100 are not known but may be an improved solubility or activation of the enzyme. In the case of human PhGPX, Triton X-100 specifically stimulated the reduction of phosphatidylcholine hydroperoxide, which was interpreted as a consequence of the transformation of the lipid bilayer into a solution of mixed micelles (40). Because the effect of Triton was not observed with H_2O_2, cumene hydroperoxide, *t*-butyl hydroperoxide, or linoleic acid hydroperoxide, a general activation of PhGPX was excluded (37). The activity of the parasite peroxidase with phosphatidylcholine hydroperoxide is very low when compared with the other hydroperoxides studied. Thus the *T. brucei* enzyme clearly differs in its substrate preference from *T. cruzi* glutathione peroxidase I and the mammalian PhGPX. With 0.1% Triton X-100 in the assay, the latter enzyme shows a significantly higher activity with phosphatidylcholine hydroperoxide than with H_2O_2 (39). *T. cruzi* glutathione peroxidase I reduces phosphatidylcholine hydroperoxide but does not accept H_2O_2 as substrate (12).

Quantification and Subcellular Localization of the Peroxidase(s) in Bloodstream and Procyclic T. brucei—On chromosome 7, *T. brucei* encodes three nearly identical genes for cysteine homologues of glutathione peroxidases. Western blot analysis with polyclonal antibodies against the recombinant His_6-peroxidase III revealed a single protein band in both bloodstream and procyclic *T. brucei* (14). Purification of the recombinant tag-free protein allowed us to estimate the cellular concentration of the enzyme. Western blots with 1×10^6 and 2×10^6 parasites in comparison with different amounts of

[3] R. Brigelius-Flohé, personal communication.

TABLE I
Apparent rate constants of T. brucei peroxidase III for the reduction of different hydroperoxides with the trypanothione/tryparedoxin system as reducing substrate

The Dalziel coefficients Φ_1 and Φ_2 for linoleic acid hydroperoxide and thymine hydroperoxide are the means of two and three independent series, respectively. The Φ_1 coefficients were determined in the case of linoleic acid hydroperoxide for four concentrations and with thymine hydroperoxide for five different concentrations of tryparedoxin. Φ_1 and Φ_2 correspond to the reciprocal of the apparent rate constants k_1' and k_2' for the two half reactions. k_1' is $k_{+1} - k_{-1}$ and may be regarded as k_{+1} because the partial reaction should be irreversible. $Peroxidase_{red}$ + ROOH → $peroxidase_{ox}$ + ROH + H_2O ($k_1' = 1/\Phi_1$). k_2' is the overall rate constant for the two-step regeneration of reduced enzyme by tryparedoxin. $Peroxidase_{ox}$ + $tryparedoxin_{red}$ → $peroxidase_{red}$ + $tryparedoxin_{ox}$ ($k_2' = 1/\Phi_2$). The extrapolated Φ_0 coefficients were zero within the experimental error. No limiting K_m values, given as Φ_1/Φ_0 and Φ_2/Φ_0, were obtained for all hydroperoxide substrates studied.

Hydroperoxide	Φ_0	Φ_1	k_1'	Φ_2	k_2'
	s	$\mu M \times s$	$M^{-1} s^{-1} \times 10^4$	$\mu M \times s$	$M^{-1} s^{-1} 10^5$
Cumene hydroperoxide [a]	0	9.7 ± 2.1	10.3	4.75 ± 2.1	2.1
H_2O_2 [a]	0	11.5 ± 1.8	8.7	5.6	1.8
Thymine hydroperoxide	0	13.2 ± 2.8	7.6	3.5 ± 0.5	2.8
Linoleic acid hydroperoxide	0	25 ± 6	4	4 ± 0.2	2.5
t-Butyl hydroperoxide [a]	0	81 ± 43	1.2	4.2 ± 2.1	2.4

[a] From Hillebrand *et al.* (14).

TABLE II
Specific activity of T. brucei Px III for different hydroperoxide substrates in the absence and presence of 0.1% Triton X-100

The assays contained 100 μM trypanothione, 10 μM tryparedoxin, and 50 μM hydroperoxide substrate as described under "Experimental Procedures." Reaction mixtures without hydroperoxide but containing 0.1 and 0.3% Triton X-100 served as controls. The activities are the mean of triplicate measurements that differed by less than 10%.

Hydroperoxide	Triton X-100	
	None	0.1%
	units/mg	
H_2O_2	3.8	7.0
Thymine hydroperoxide	4.2	7.5
Linoleic acid hydroperoxide	1.4	4.5
t-Butyl hydroperoxide	1.1	1.8
Phosphatidylcholine hydroperoxide	0.1	1.2

the recombinant protein yielded 22 μM peroxidase in bloodstream *T. brucei* using a cell volume of 58 femtoliters (34, 41) for calculation. For procyclic cells, a cell volume of 100 femtoliters was assumed that resulted in a cellular enzyme concentration of about 10 μM (Fig. 2). This analysis does not allow us to distinguish between the probable expression of the individual peroxidases I-III that consist of 166, 169, and 169 (after cleavage of the presumed mitochondrial targeting sequence) amino acid residues, respectively.

In addition to the putative mitochondrial signal peptide, Px III has a C-terminal ARL motif that may represent a glycosomal-targeting signal. The other two proteins lack known signal sequences (14). To determine the subcellular localization of the peroxidase(s), immunofluorescence microscopy was performed on bloodstream and procyclic cells using aldolase and MitotrackerRed (Molecular Probes) as glycosomal and mitochondrial markers, respectively. The staining pattern of the peroxidase was comparable with that of tryparedoxin (data not shown). Tryparedoxin was found to be mainly cytosolic in both procyclic and bloodstream *T. brucei,* although immune electron microscopy showed some gold particles in the mitochondria (11). From these data the glutathione peroxidase-type enzyme(s) appears to be mainly cytosolic. To confirm the cytosolic localization and to assess possible additional localizations, subcellular fractions were prepared. Procyclic and bloodstream parasites were disintegrated by grinding with silicon carbide. After centrifugation, the resulting lysates were subjected to sucrose gradient centrifugation. Different cell compartments were identified by Western blots with antibodies against Pex11, a glycosomal membrane protein, against lipoamide dehydrogenase, a soluble mitochondrial enzyme, and against the endoplasmic reticulum chaperon BiP and the cytosolic trypanothione reductase. As shown in Fig. 3*A*, the peroxidases were detectable in fractions 36–50 of the bloodstream gradient in accordance with a cytosolic and mitochondrial localization with most of the protein in the cytosol. Also in procyclic *T. brucei*, the peroxidases co-eluted with trypanothione reductase and lipoamide dehydrogenase and, thus, occur in the cytosol and mitochondrion (Fig. 3*B*).

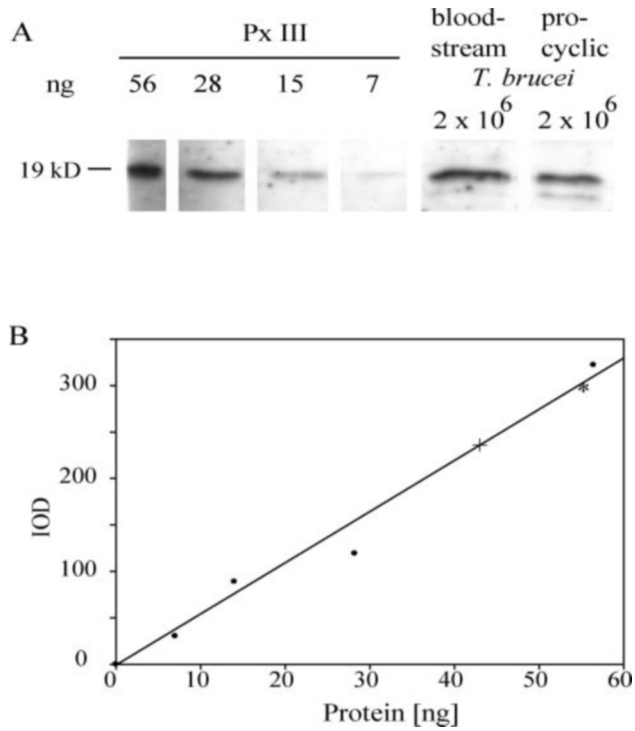

FIG. 2. **Quantification of the peroxidases in bloodstream and procyclic *T. brucei*.** *A*, Western blot analysis of total cell lysates from cultured bloodstream and procyclic *T. brucei* and 7, 15, 28, and 56 ng of tag-free recombinant peroxidase III. Polyclonal antibodies against the peroxidase together with the SuperSignal West Pico chemiluminescent substrate were used for visualization as described under "Experimental Procedures". *B*, standard diagram based on four different amounts of the recombinant protein (●) using the program GelPro Analyzer 3.1. +, 2×10^6 procyclic parasites; *, 2×10^6 bloodstream parasites. *IOD*, integrated optical density.

The Peroxidases Are Essential for T. brucei—For RNA interference experiments, two copies of a 452-bp fragment of the peroxidase gene were cloned in sense and antisense orientation on either side of a stuffer sequence in the vector pHD678. Bloodstream and procyclic *T. brucei* 449 cells were transfected

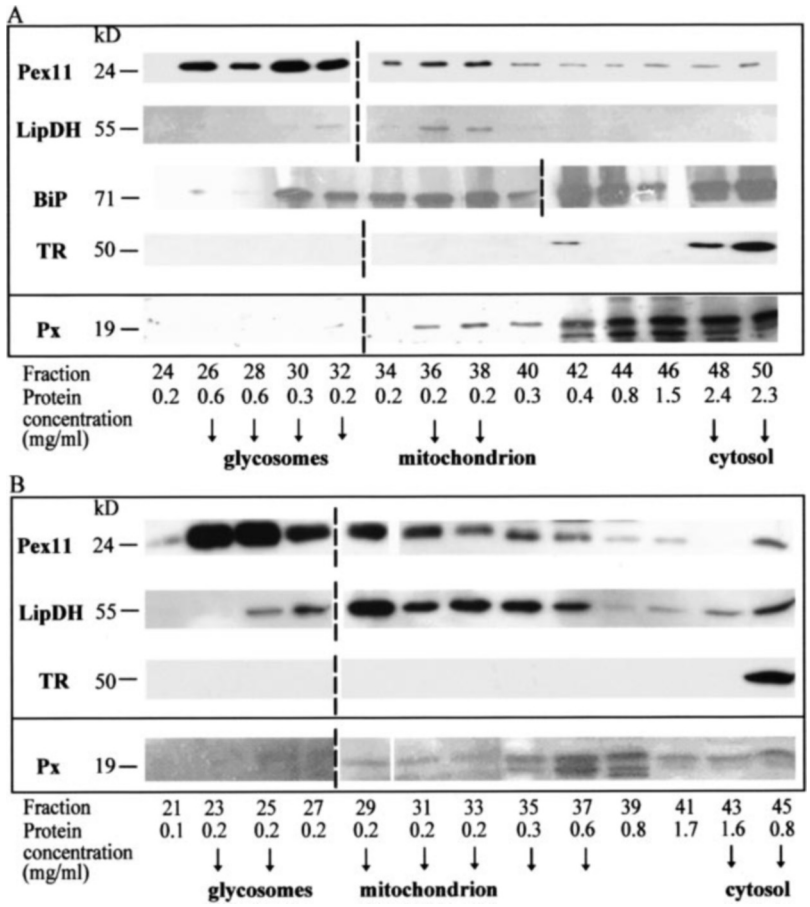

FIG. 3. **Subcellular localization of the peroxidases in bloodstream and procyclic *T. brucei brucei*.** *A*, Western blot analysis of subcellular fractions of bloodstream cells with antibodies against Pex11, lipoamide dehydrogenase, and trypanothione reductase identified 26–32 as the main glycosomal fractions, fractions 36–38 as peak mitochondrial fractions, and the cytosol starting with fraction 48, respectively. Antibodies against the endoplasmic reticulum matrix protein BiP recognized the protein starting with fraction 30 nearly throughout the gradient. The peroxidases were detectable in the cytosolic and mitochondrial fractions. *B*, Western blots of subcellular fractions of procyclic cells showed the glycosomal Pex11 in fractions 23–31, the mitochondrial lipoamide dehydrogenase (*LipDH*) mainly in fractions 29–37 and the cytosolic TR from fraction 43 onward. Also in procyclic cells, the peroxidases are detectable in the cytosol and mitochondrion. The bands of Pex11 and lipoamide dehydrogenase in fraction 45 of the procyclic gradient are probably due to some broken organelles. The *bands below* the peroxidase are caused by cross-reactions with other cytosolic proteins. The protein concentration of the unconcentrated fractions are given in mg/ml. For each protein to be analyzed, two gels were run in parallel and developed together under identical conditions. A *dotted line* is drawn between the two gels.

(Figs. 4 and 5), and generation of a double-stranded hairpin RNA was induced by the addition of tetracycline. Three bloodstream and procyclic clones were analyzed in detail and showed very similar results. Northern blot analyses yielded a prominent mRNA of about 1000 bp and a faint band of 1400 bp in both cell types. In cells transfected with pHD678*px*, the addition of tetracycline led to the disappearance of both mRNAs, whereas the control tubulin mRNAs were detectable in equal amounts independent of tetracycline (Figs. 4*A* and 5*A*). Protein expression of the peroxidases was down-regulated to ≤5% after tetracycline addition as shown by Western blot analyses (Figs. 4*B* and 5*B*). TR served as the loading control and was present in equal amounts independent of tetracycline. Cell growth of the RNA interference clones was studied in two models. In the first approach, RNA interference was induced once with 0.5 or 1 μg/ml tetracycline, and the parasites were cultivated for at least 72 h to obtain sufficient material for Northern blot analyses. The cell density was monitored microscopically every 24 h. In a second series, to exclude growth defects as a result of overgrowing cells and to follow cell growth over a longer time period, tetracycline was added every 24 h, and the parasite cultures were diluted each time to resume the starting cell density. In both models, bloodstream and procyclic *T. brucei* cells showed a significantly impaired growth behavior upon tetracycline addition (Figs. 4, *C* and *D*, and 5, *C* and *D*). In procyclic cells, growth retardation became obvious 24 h after induction, whereas in bloodstream cells, depending on the cultivation model, it took 48–72 h to develop severe growth defects. Interestingly, in procyclic cells, after 6 days of cultivation in 24 h cycles growth of the clones became independent of the presence of tetracycline (Fig. 5*D*). An identical behavior was observed when procyclic parasites cultivated for 140 h were diluted to a density of 1×10^6 cells/ml. After 24 h the clones shown in Fig. 5*C* grew normally independent of tetracycline (data not shown). Such phenomena have been reported previously for other essential proteins in *T. brucei*. Examples are the glycosomal membrane protein Pex14 (42), the zinc finger protein TbMP81 required for RNA editing in bloodstream and procyclic *T. brucei* (43), and the cytosolic 2 Cys-peroxiredoxin in bloodstream *T. brucei* (17). It was attributed to a genetic or epigenetic escape from the inducible RNA interference system (42) or to a genetic or physiological compensation for the loss of the protein. The latter explanation is not valid for the peroxidase(s) studied here since recovery of the growth rate was accompanied by the re-appearance of the mRNAs and protein (data not shown). For bloodstream cells, no recovery after the knock-down of the peroxidases was observed after 6 days of continuous cultivation in the presence of 0.5 μg/ml tetracycline in accordance with data obtained by Wilkinson *et al.* (17). Procyclic and bloodstream cells transfected with the empty expression plasmid showed identical amounts of peroxidase mRNA and protein independent of tetracycline, and their growth behavior with and without 0.5 or 1 μg/ml tetracycline was indistinguishable from that of wild-type 449 cells. In conclusion, the growth defects observed upon induction of RNA interference are due to the specific depletion of the peroxidases. The data clearly show that the glutathione peroxidase-type tryparedoxin peroxidases are essential in both the mammalian and insect stages of the parasite.

DISCUSSION

The glutathione peroxidase-type *T. brucei* tryparedoxin peroxidase studied here readily reduces H_2O_2, thymine hydroperoxide, and linoleic acid hydroperoxide, which probably repre-

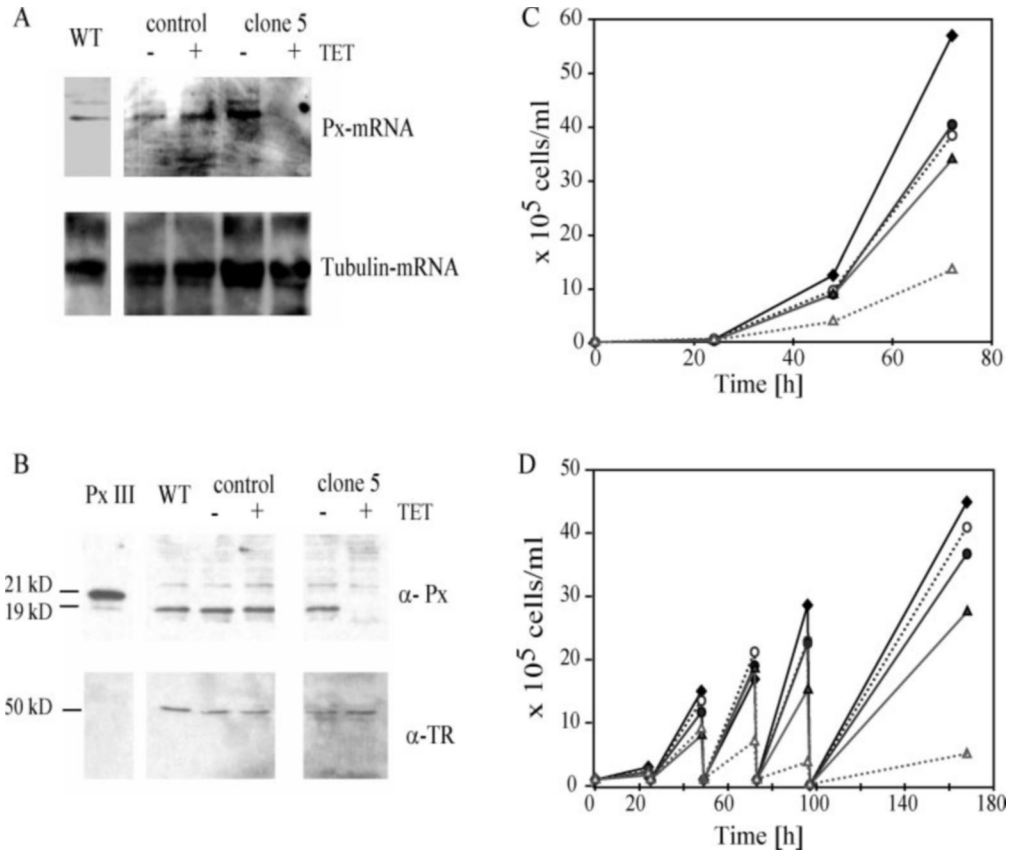

FIG. 4. **Tetracycline (*TET*)-induced RNA-interference response in bloodstream *T. brucei brucei.*** Wild-type (*WT*) bloodstream BF449 cells ((◆, −*TET*) and control BF449 cells with pHD678 (●, −*TET*; ○, +*TET*) were compared with BF449 containing pHD678*px*, clone 5 (▲, −*TET*; △, +*TET*). *A*, Northern blot analysis. The culture was diluted to 2×10^4 cells/ml, RNA interference was induced with 0.5 μg/ml tetracycline, and the cells were harvested after 72 h of continuous cultivation. 7 μg of total RNA from 5×10^8 cells was applied per lane. The peroxidase mRNA was hybridized with a digoxigenin-labeled probe of the *px*-coding region as described under "Experimental Procedures." A digoxigenin-labeled probe against β-tubulin served as a loading control. *B*, Western blot analysis. 1×10^5 cells/ml were induced with 1 μg/ml tetracycline, and after 72 h of cultivation in 24 h cycles, 2×10^6 cells were applied per lane. The peroxidases were detected by the polyclonal rabbit antiserum against Px III (1:1000). As a loading control, the blots were stripped and developed with the purified TR antibodies (1:500). *C*, growth curves of continuously cultivated bloodstream parasites. The cultures were diluted to 2×10^5 cells/ml, and RNA interference was induced by adding 0.5 μg/ml tetracycline. The cell density was monitored every 24 h over 3 days. *D*, growth curves of cells cultivated in 24-h cycles. Bloodstream parasites were diluted to 1×10^5 cells/ml, 1 μg/ml tetracycline was added, and the cultures were diluted every 24 h to the starting cell density.

sent physiological substrates. In contrast, phosphatidylcholine hydroperoxide is a very poor substrate and, in the absence of detergent, even an inhibitor of the enzyme. The *T. brucei* enzyme is the first trypanosomatid peroxidase shown to reduce thymine hydroperoxide. This model compound for DNA oxidative damage is an excellent substrate of human phospholipid hydroperoxide glutathione peroxidase, and a role of the enzyme in the repair of oxidatively damaged DNA has been suggested (44). Thymine hydroperoxide is not reduced by the cytosolic mammalian GPX. Of the four mammalian selenoglutathione peroxidases, PhGPX is the most similar of the *T. brucei* enzyme. The two enzymes show an overall sequence identity of 39% and are monomeric proteins. In addition, both peroxidases occur in the cytosol and mitochondria (39, 45). PhGPX accepts a broad spectrum of hydroperoxides, particularly fatty acid and phospholipid hydroperoxides (19, 37, 46). This lack of substrate specificity has been attributed to the fact that PhGPX acts as a monomer, whereas the other mammalian glutathione peroxidases are tetrameric proteins (47). Because the *T. brucei* peroxidase as well as a cysteine-containing glutathione peroxidase from *P. falciparum* (21) are also monomeric but do not reduce phosphatidylcholine hydroperoxide, it is unlikely that the broad specificity of the PhGPX is mainly due to a better accessibility of its redox center.

The closest relative of the *T. brucei* peroxidase is a *T. cruzi* enzyme first described as glutathione peroxidase I (12) and later shown also to prefer the trypanothione/tryparedoxin system as electron source (13). *T. cruzi* glutathione peroxidase I has been reported to be encoded by a single copy gene (12). This is not the case. In *T. cruzi*, as is the case in *T. brucei* and *L. major*, a genomic locus encodes a cluster of three, at least 95% identical genes. Despite this conserved genomic organization and an amino acid sequence identity of 72%, the T. *brucei* and *T. cruzi* peroxidases have remarkably different substrate specificities. In contrast to the *T. brucei* peroxidase studied here, the *T. cruzi* enzyme does not accept H_2O_2 (12, 13) but prefers fatty acid and phospholipid hydroperoxides. The assumption that the *T. brucei* peroxidase behaves like the *T. cruzi* glutathione peroxidase I and is mainly engaged in the removal of oxidatively damaged lipids (17) is, therefore, unlikely. There is some evidence for a general function of the *T. cruzi* peroxidase in oxidative defense since overexpression of the enzyme conferred a slight increase in resistance toward exogenous H_2O_2 and *t*-butyl hydroperoxide (13), but a direct role in membrane protection has yet to be shown. The subcellular distribution of these peroxidases in African and American trypanosomes is also remarkably different. *T. cruzi* glutathione peroxidase I has been reported to occur in glycosomes and the cytosol (13). In contrast, the *T. brucei* glutathione peroxidase-type enzymes described here are detectable in the cytosol and

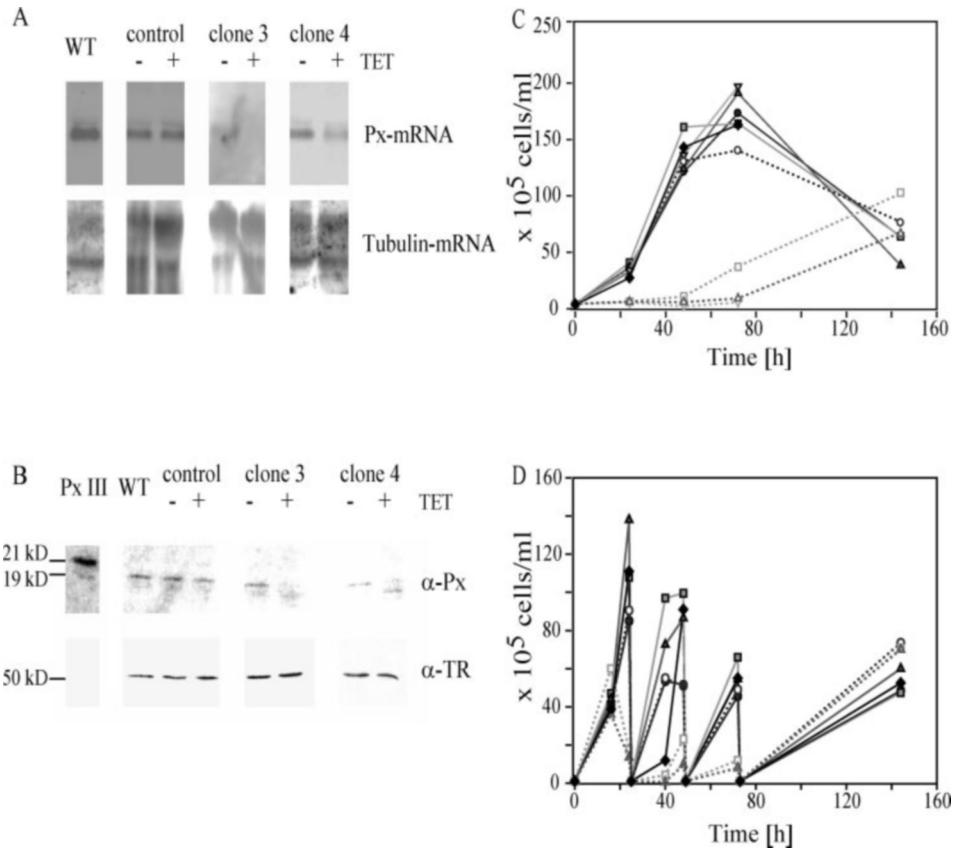

FIG. 5. **Tetracycline (*TET*)-induced RNA-interference response in procyclic *T. brucei brucei*.** Wild-type (*WT*) procyclic PC449 cells (◆, −*TET*) and control PC449 cells with pHD678, (●, −*TET*; ○, +*TET*) were compared with three tetracycline-induced and non-induced clones of PC449 containing pHD678*px,* clone 2 (*gray box*, −*TET*; *open square*, +*TET*), clone 3 (▲, −TET; △, +TET), clone 4 (*light gray inverted triangle*, −*TET*; *open inverted triangle*, +*TET*). *A*, Northern blot analysis. A culture with 4×10^5 cells/ml was induced with 1 μg/ml tetracycline, and the cells were harvested after 24 h (*control*, *clone 4*) or 48 h (*clone 3*). 12–15 μg of total RNA from 5×10^8 cells was applied per *lane*. B, Western blot analysis. Total cell lysate from 2×10^6 cells was applied per lane. 4×10^5 cells/ml were treated with 1 μg/ml tetracycline, and the cells were harvested after 24 h. *C*, growth curves of continuously cultivated parasites. A cell culture with 4×10^5 cells/ml was induced with 1 μg/ml tetracycline, and the cells were cultivated for 72 h. *D*, growth curves of cells cultivated in 24-h cycles. 1×10^6 cells/ml were treated daily with 1 μg/ml tetracycline for a 6-day period. For details see the legend of Fig. 4 and "Experimental Procedures."

mitochondria but not the glycosomes of bloodstream and procyclic parasites. This subcellular localization coincides with that of the parasite peroxiredoxins (11).

Besides the N-terminal mitochondrial signal sequence, *T. brucei* peroxidase III has a putative C-terminal peroxisomal targeting signal. The sole mitochondrial and cytosolic localization of the enzyme in bloodstream and procyclic cells indicates that the peroxisomal targeting signal must have been repressed in some way. Studies on mammalian proteins revealed that in many cases the mitochondrial signal sequence is functionally dominant (48). One explanation is that the mitochondrial signal, which is translated first, causes the protein to be immediately recognized and translocated into the mitochondrion. Another possibility has been reported in the case of the rat liver pyruvate/alanine glyoxylate aminotransferase. Here the presence of the mitochondrial-targeting signal causes the protein to become unfolded, which represses the peroxisomal targeting signal (49). The putative mitochondrial signal peptide of *T. brucei* peroxidase III is only seven residues long. Such exceptionally short targeting sequences have been observed in other trypanosomatid proteins (50). In the Western blots of the mitochondrial and cytosolic fractions of the cell gradient the size of the protein bands was indistinguishable, suggesting cleavage of the leader sequence in Px III.

Depletion of the glutathione peroxidase-type enzyme(s) causes severe growth defects in bloodstream and procyclic *T. brucei*. The same is true for the cytosolic 2 Cys-peroxiredoxin in bloodstream cells (17). Obviously the two types of peroxidases cannot functionally substitute for each other. In the insect trypanosomatid *Crithidia fasciculata*, cytosolic peroxiredoxin represents about 6% of the total soluble protein and, thus, is an extremely abundant protein (10). If this is also the case in *T. brucei*, the cellular concentration of the peroxiredoxin would be at least an order of magnitude higher than that of the glutathione peroxidase-type enzymes. The fact that the latter enzymes are nevertheless essential strongly argues for physiological roles different from a general defense against oxidative stress. This assumption is in agreement with data from Wilkinson *et al.* (17), where the H_2O_2 sensitivity of bloodstream cells depleted of the mitochondrial and cytosolic peroxiredoxins as well as the glutathione peroxidase-type enzyme was studied. Only depletion of the cytosolic 2 Cys-peroxiredoxin increased the sensitivity of the parasites toward exogenous H_2O_2. In mammalian cells, peroxiredoxins are both peroxide-destroying enzymes and peroxide targets being over-oxidized (51). The latter property is presumably not valid for the kinetoplastid peroxiredoxins (52), but the cytosolic peroxiredoxin obviously plays the major role in the defense against exogenous oxidative stress. The fact that the intracellular concentration of the glutathione peroxidase-type enzymes is probably more than an order of magnitude lower than that of the peroxiredoxins and that in general the cysteine homologues of the classical glutathione peroxidases have much lower activities than the mammalian seleno-enzymes support the assumption that these

enzymes have specialized functions. Although the RNA interference approach could not discriminate between the cytosolic and mitochondrial enzymes, one may speculate that the mitochondrial glutathione peroxidase-type enzyme plays an important role because the mitochondrial peroxiredoxin proved to be not essential (17). The source of reducing equivalents for the mitochondrial peroxidases remains unclear because trypanothione reductase has been found only in the cytosol of *T. brucei* (53) (Figs. 4 and 5). There may be some mitochondrial tryparedoxin. Immunofluorescence showed only a cytosolic localization, but immune electron microscopy studies displayed some tryparedoxin also in the mitochondrion (11). The presence of a second tryparedoxin in *T. brucei* has been reported (17), but no localization studies were performed so far.

Thymine hydroperoxide is an excellent substrate of Px III, which may indicate a function of the enzyme in the protection of mitochondrial DNA against oxidative stress as was proposed for mammalian PhGPX (44). Mitochondrial DNA is much more sensitive to oxidative damage than nuclear DNA (54). The peroxidase could also be involved in redox regulation processes. In *C. fasciculata* tryparedoxin activates the binding of a universal minicircle sequence-binding protein at the kinetoplast DNA, and it was postulated that tryparedoxin-dependent peroxidases could regulate the redox state of tryparedoxin and, thus, influence this replication initiation process (6). Another possible reason for the requirement of both types of tryparedoxin peroxidases are different physiological substrate preferences. Only H_2O_2, *t*-butyl hydroperoxide, and cumene hydroperoxide have been studied as substrates of the cytosolic peroxiredoxin, and the mitochondrial peroxiredoxin has so far only been shown to reduce hydrogen peroxide (11). There is evidence for a role of the peroxiredoxins in the detoxification of peroxynitrite. The cytosolic *T. cruzi* and *T. brucei* 2 Cys-peroxiredoxins reduce peroxynitrite with second order rate constants of about 8×10^5 M^{-1} s^{-1} (55). It will be interesting to study if the glutathione peroxidase-type tryparedoxin peroxidases also catalyzes reduction of peroxynitrite.

Of the four selenocysteine-containing glutathione peroxidases in mammals, only the cytosolic GPX I appears to fight a generalized oxidative stress (18). For PhGPX, several functions independent of oxidative defense have been proposed such as regulation of differentiation and proliferation processes (38), modulation of gene expression (56), or acting as a structural protein (45). Peroxidases probably play a general role in redox regulation mechanisms by balancing the hydroperoxide levels in the cell and, thus, causing the direct activation or inactivation of specific proteins.

In *T. brucei*, reactive oxygen species activate an apoptosis-like Ca^{2+}-dependent cell death pathway (57). In mammalian cells, overexpression of GPX I or PhGPX, particularly if the latter protein is targeted to mitochondria, inhibits apoptosis (18). Depletion of a mitochondrial-specific peroxiredoxin in HeLa cells resulted in increased levels of H_2O_2 and sensitized the cells to induction of apoptosis (58). Under oxidative stress it is likely that all parasite peroxidases are able to detoxify hydroperoxides. But under normal culture conditions a certain peroxide level might be important to maintain regulatory processes or the mitochondrial structure. Because the mitochondrial 2 Cys-peroxiredoxin is not essential even under oxidative stress conditions, one may speculate that the glutathione peroxidase-type plays an important role for the organelle. A recent study on the role of alternative oxidase in *T. brucei* indicated that this mitochondrial enzyme is involved in the defense against oxidative stress. In addition, the data showed that even in the bloodstream mitochondrion, which lacks oxidative phosphorylation, low levels of H_2O_2 are constantly produced (59). The mitochondrial peroxidase may, thus, play a role in balancing the peroxide level in this organelle.

Acknowledgments—We thank Dr. James Bangs, Bardeen Medical Laboratories, Madison WI, for providing polyclonal rabbit antibodies against *T. brucei* BiP. Dr. Regina Brigelius-Flohé, German Institute of Human Nutrition, Potsdam, Germany is acknowledged for a kind gift of phosphatidylcholine hydroperoxide and rat phospholipid glutathione peroxidase.

REFERENCES

1. Fairlamb, A. H., and Cerami, A. (1992) *Annu. Rev. Microbiol.* **46,** 695–729
2. Tabor, H., and Tabor, C. W. (1975) *J. Biol. Chem.* **250,** 2648–2654
3. Schmidt, H., and Krauth-Siegel, R. L. (2003) *J. Biol. Chem.* **278,** 46329–46336
4. Dormeyer, M., Reckenfelderbäumer, N., Lüdemann, H., and Krauth-Siegel, R. L. (2001) *J. Biol. Chem.* **276,** 10602–10606
5. Vickers, T. J., Wyllie, S. H., and Fairlamb, A. H. (2004) *J. Biol. Chem.* **279,** 49003–49009
6. Onn, I., Milman-Shtepel, N., and Shlomai, J. (2004) *Eukaryot. Cell* **3,** 277–287
7. Irsch, T., and Krauth-Siegel, R. L. (2004) *J. Biol. Chem.* **279,** 22209–22217
8. Müller, S., Liebau, E., Walter, R. D., and Krauth-Siegel, R. L. (2003) *Trends Parasitol.* **19,** 320–328
9. Flohé, L., Steinert, P., Hecht, H. J., and Hofmann, B. (2002) *Methods Enzymol.* **347,** 244–258
10. Nogoceke, E., Gommel, D. U., Kiess, M., Kalisz, H. M., and Flohé, L. (1997) *Biol. Chem.* **378,** 827–836
11. Tetaud, E., Giroud, C., Prescott, A. R., Parkin, D. W., Baltz, D., Biteau, N., Baltz, T., and Fairlamb, A. H. (2001) *Mol. Biochem. Parasitol.* **116,** 171–183
12. Wilkinson, S. R., Meyer, D. J., and Kelly, J. M. (2000) *Biochem. J.* **352,** 755–761
13. Wilkinson, S. R., Meyer, D. J., Taylor, M. C., Bromley, E. V., Miles, M. A., and Kelly, J. M. (2002) *J. Biol. Chem.* **277,** 17062–17071
14. Hillebrand, H., Schmidt, A., and Krauth-Siegel, R. L. (2003) *J. Biol. Chem.* **278,** 6809–6815
15. Wilkinson, S. R., Obado, S. O., Mauricio, I. L., and Kelly, J. M. (2002) *Proc. Natl. Acad. Sci. U. S. A.* **99,** 13453–13458
16. Gommel, D. U., Nogoceke, E., Morr, M., Kiess, M., Kalisz, H. M., and Flohé, L. (1997) *Eur. J. Biochem.* **248,** 913–918
17. Wilkinson, S. R., Horn, D., Prathalingam, S. R., and Kelly, J. M. (2003) *J. Biol. Chem.* **278,** 31640–31646
18. Brigelius-Flohé, R., and Flohé, L. (2003) *Biofactors* **17,** 93–102
19. Björnstedt, M., Xue, J., Huang, W., Akesson, B., and Holmgren, A. (1994) *J. Biol. Chem.* **269,** 29382–29384
20. Williams, D. L., Pierce, R. J., Cookson, E., and Capron, A. (1992) *Mol. Biochem. Parasitol.* **52,** 127–130
21. Sztajer, H., Gamain, B., Aumann, K. D., Slomianny, C., Becker, K., Brigelius-Flohé, R., and Flohé, L. (2001) *J. Biol. Chem.* **276,** 7397–7403
22. Tang, L., Gounaris, K., Griffiths, C., and Selkirk, M. E. (1995) *J. Biol. Chem.* **270,** 18313–18318
23. Lüdemann, H., Dormeyer, M., Sticherling, C., Stallmann, D., Follmann, H., and Krauth-Siegel, R. L. (1998) *FEBS Lett.* **431,** 381–385
24. Sullivan, F. X., and Walsh, C. T. (1991) *Mol. Biochem. Parasitol.* **44,** 145–147
25. Reckenfelderbäumer, N., and Krauth-Siegel, R. L. (2002) *J. Biol. Chem.* **277,** 17548–17555
26. Lorenz, P., Maier, A. G., Baumgart, E., Erdmann, R., and Clayton, C. (1998) *EMBO J.* **17,** 3542–3555
27. Schöneck, R., Billaut-Mulot, O., Numrich, P., Ouaissi, M. A., and Krauth-Siegel, R. L. (1997) *Eur. J. Biochem.* **243,** 739–747
28. Hahn, B. S., and Wang, S. Y. (1976) *J. Org. Chem.* **41,** 567–568
29. Gibian, M. J., and Vandenberg, P. (1987) *Anal. Biochem.* **163,** 343–349
30. Dalziel, K. (1957) *Acta Chem. Scand.* **11,** 1706–1723
31. Forstrom, J. W., Stults, F. H., and Tappel, A. L. (1979) *Arch. Biochem. Biophys.* **193,** 51–55
32. Cunningham, M. P., and Vickerman, K. (1962) *Trans. R. Soc. Trop. Med. Hyg.* **56,** 48–59
33. Biebinger, S., Wirtz, L. E., Lorenz, P., and Clayton, C. (1997) *Mol. Biochem. Parasitol.* **85,** 99–112
34. Opperdoes, F. R., Baudhuin, P., Coppens, I., De Roe, C., Edwards, S. W., Weijers, P. J., and Misset, O. (1984) *J. Cell Biol.* **98,** 1178–1184
35. Shi, H., Djikeng, A., Mark, T., Wirtz, E., Tschudi, C., and Ullu, E. (2000) *RNA (N. Y.)* **6,** 1069–1076
36. Wang, Z., Morris, J. C., Drew, M. E., and Englund, P. T. (2000) *J. Biol. Chem.* **275,** 40174–40179
37. Ursini, F., Maiorino, M., and Gregolin, C. (1985) *Biochim. Biophys. Acta* **839,** 62–70
38. Roveri, A., Maiorino, M., and Ursini, F. (1994) *Methods Enzymol.* **233,** 202–212
39. Maiorino, M., Gregolin, C., and Ursini, F. (1990) *Methods Enzymol.* **186,** 448–457
40. Ursini, F., Maiorino, M., and Gregolin, C. (1986) *Int. J. Tissue React.* **8,** 99–103
41. Grünfelder, C. G., Engstler, M., Weise, F., Schwarz, H., Stierhof, Y. D., Boshart, M., and Overath, P. (2002) *Traffic* **3,** 547–559
42. Furuya, T., Kessler, P., Jardim, A., Schnaufer, A., Crudder, C., and Parsons, M. (2002) *Proc. Natl. Acad. Sci. U. S. A.* **99,** 14177–14182
43. Drozdz, M., Palazzo, S. S., Salavati, R., O'Rear, J., Clayton, C., and Stuart, K. (2002) *EMBO J.* **21,** 1791–1799
44. Bao, Y., Jemth, P., Mannervik, B., and Williamson, G. (1997) *FEBS Lett.* **410,** 210–212
45. Ursini, F., Heim, S., Kiess, M., Maiorino, M., Roveri, A., Wissing, J., and Flohé, L. (1999) *Science* **285,** 1393–1396
46. Ursini, F., Maiorino, M., Brigelius-Flohé, R., Aumann, K. D., Roveri, A., Schomburg, D., and Flohé, L. (1995) *Methods Enzymol.* **252,** 38–53

47. Brigelius-Flohé, R., Aumann, K. D., Blöcker, H., Gross, G., Kiess, M., Klöppel, K. D., Maiorino, M., Roveri, A., Schuckelt, R., Ursini, F., Wingender, E., and Flohé, L. (1994) *J. Biol. Chem.* **269,** 7342–7348
48. Oatey, P. B., Lumb, M. J., and Danpure, C. J. (1996) *Eur. J. Biochem.* **241,** 374–385
49. Oda, T., Uchida, C., and Miura, S. (2000) *J. Biochem.* (*Tokyo*) **127,** 665–671
50. Häusler, T., Stierhof, Y. D., Blattner, J., and Clayton, C. (1997) *Eur. J. Cell Biol.* **73,** 240–251
51. Rabilloud, T., Heller, M., Gasnier, F., Luche, S., Rey, C., Aebersold, R., Benahmed, M., Louisot, P., and Lunardi, J. (2002) *J. Biol. Chem.* **277,** 19396–19401
52. Wood, Z. A., Poole, L. B., and Karplus, P. A. (2003) *Science* **300,** 650–653
53. Smith, K., Opperdoes, F. R., and Fairlamb, A. H. (1991) *Mol. Biochem. Parasitol.* **48,** 109–112
54. Yakes, F. M., and Van Houten, B. (1997) *Proc. Natl. Acad. Sci. U. S. A.* **94,** 514–519
55. Trujillo, M., Budde, H., Pineyro, M. D., Stehr, M., Robello, C., Flohé, L., and Radi, R. (2004) *J. Biol. Chem.* **279,** 34175–34182
56. Kitahara, J., Chiba, N., Sakamoto, H., and Nakagawa, Y. (2003) *Gene. Expr.* **11,** 77–83
57. Ridgley, E. L., Xiong, Z. H., and Ruben, L. (1999) *Biochem. J.* **340,** 33–40
58. Chang, T. S., Cho, C. S., Park, S., Yu, S., Kang, S. W., and Rhee, S. G. (2004) *J. Biol. Chem.* **279,** 41975–41984
59. Fang, J., and Beattie, D. S. (2003) *Arch. Biochem. Biophys.* **414,** 294–302